Original Article

Imaging of the extracranial internal carotid artery in acute ischemic stroke: assessment of stenosis, plaques, and image quality using relaxation-enhanced angiography without contrast and triggering (REACT)

Ulrike Cornelia Isabel Hoyer[1], Simon Lennartz[1], Nuran Abdullayev[1], Florian Fichter[1], Stephanie T. Jünger[2], Lukas Goertz[1,2], Kai Roman Laukamp[1], Roman Johannes Gertz[1], Jan-Peter Grunz[3], Christopher Hohmann[4], David Maintz[1], Thorsten Persigehl[1], Christoph Kabbasch[1], Jan Borggrefe[1,5], Kilian Weiss[6], Lenhard Pennig[1]

[1]Institute for Diagnostic and Interventional Radiology, Faculty of Medicine and University Hospital Cologne, University of Cologne, Cologne, Germany; [2]Department of General Neurosurgery, Center for Neurosurgery, Faculty of Medicine and University Hospital Cologne, University of Cologne, Cologne, Germany; [3]Department of Diagnostic and Interventional Radiology, University Hospital Würzburg, Würzburg, Germany; [4]Department III of Internal Medicine, Heart Center, Faculty of Medicine and University Hospital Cologne, University of Cologne, Cologne, Germany; [5]Department of Radiology, Neuroradiology and Nuclear Medicine, Johannes Wesling University Hospital, Ruhr University Bochum, Bochum, Germany; [6]Philips GmbH, Hamburg, Germany

Contributions: (I) Conception and design: L Pennig, J Borggrefe, C Kabbasch, K Weiss, UCI Hoyer, T Persigehl, S Lennartz, C Hohmann; (II) Administrative support: D Maintz, T Persigehl, C Kabbasch, J Borggrefe, K Weiss; (III) Provision of study materials or patients: L Pennig; (IV) Collection and assembly of data: L Pennig, J Borggrefe, C Kabbasch, K Weiss, T Persigehl, JP Grunz; (V) Data analysis and interpretation: UCI Hoyer, N Abdullayev, F Fichter, S Lennartz, L Goertz, ST Jünger, KR Laukamp, RJ Gertz; (VI) Manuscript writing: All authors; (VII) Final approval of manuscript: All authors.

Correspondence to: Lenhard Pennig, MD. Institute for Diagnostic and Interventional Radiology, Faculty of Medicine and University Hospital Cologne, University of Cologne, Kerpener Straße 62, 50937 Cologne, Germany. Email: Lenhard.pennig@uk-koeln.de.

Background: In stroke magnetic resonance imaging (MRI), contrast-enhanced magnetic resonance angiography (CE-MRA) is the clinical standard to depict extracranial arteries but native MRA techniques are of increased interest to facilitate clinical practice. The purpose of this study was to assess the detection of extracranial internal carotid artery (ICA) stenosis and plaques as well as the image quality of cervical carotid arteries between a novel flow-independent relaxation-enhanced angiography without contrast and triggering (REACT) sequence and CE-MRA in acute ischemic stroke (AIS).

Methods: In this retrospective, single-center study, 105 consecutive patients (65.27±18.74 years, 63 males) were included, who received a standard stroke protocol at 3T in clinical routine including Compressed SENSE (CS) accelerated (factor 4) 3D isotropic REACT (fixed scan time: 02:46 min) and CS accelerated (factor 6) 3D isotropic CE-MRA. Three radiologists independently assessed scans for the presence of extracranial ICA stenosis and plaques (including hyper-/hypointense signal) with concomitant diagnostic confidence using 3-point scales (3= excellent). Vessel quality, artifacts, and image noise of extracranial carotid arteries were subjectively scored on 5-point scales (5= excellent/none). Wilcoxon tests were used for statistical comparison.

Results: Considering CE-MRA as the standard of reference, REACT provided a sensitivity of 89.8% and specificity of 95.2% for any and of 93.5% and 95.8% for clinically relevant (≥50%) extracranial ICA stenosis and yielded a to CE-MRA comparable diagnostic confidence [mean ± standard deviation (SD), median (interquartile range): 2.8±0.5, 3 (3–3) *vs.* 2.7±0.5, 3 (2–3), P=0.03]. Using REACT, readers detected more plaques overall (n=57.3 *vs.* 47.7, P<0.001) and plaques of hyperintense signal (n=12.3 *vs.* 5.7, P=0.02) with

higher diagnostic confidence [2.8±0.5, 3 (3–3) *vs.* 2.6±0.7, 3 (2–3), P<0.001] than CE-MRA. After analyzing a total of 1,260 segments, the vessel quality of all segments combined [4.61±0.66 *vs.* 4.58±0.68, 5 (4–5) *vs.* 5 (4–5), P=0.0299] and artifacts [4.51±0.70 *vs.* 4.44±0.73, 5 (4–5) *vs.* 5 (4–5), P>0.05] were comparable between the sequences with REACT showing a lower image noise [4.43±0.67 *vs.* 4.25±0.71, 5 (4–5) *vs.* 4 (4–5), P<0.001].

Conclusions: Without the use of gadolinium-based contrast agents or triggering, REACT provides a high sensitivity and specificity for extracranial ICA stenosis and a potential improved depiction of adjacent plaques while yielding to CE-MRA comparable vessel quality in a large patient cohort with AIS.

Keywords: Acute ischemic stroke (AIS); extracranial arteries; contrast-enhanced magnetic resonance angiography (CE-MRA); relaxation-enhanced angiography without contrast and triggering (REACT)

Submitted Nov 19, 2021. Accepted for publication Mar 22, 2022.
doi: 10.21037/qims-21-1122
View this article at: https://dx.doi.org/10.21037/qims-21-1122

Introduction

Atherosclerotic disease of the carotid arteries, e.g., internal carotid artery (ICA) stenosis or occlusion resulting from atherosclerotic plaques, represents a major cause of acute ischemic stroke (AIS) (1,2). In stroke magnetic resonance imaging (MRI), imaging of the extracranial arteries is routinely performed using contrast-enhanced magnetic resonance angiography (CE-MRA), which represents a reliable technique for the assessment of the severity of ICA stenosis (3) and allows for the detection and assessment of adjacent plaques, albeit not approximating to dedicated plaque imaging (4-6). While CE-MRA provides a fast acquisition with high isotropic spatial resolution, it is not recommended in patients with severe renal insufficiency given the risk of nephrogenic systemic fibrosis (7). Furthermore, potential allergic reactions (8) and unknown effects of gadolinium deposition in the central nervous system (9) might discourage radiologists and patients to employ CE-MRA. Occasionally, technical failure of CE-MRA, e.g., due to mistiming of the contrast bolus with respect to the center of k-space, results in insufficient contrast or venous contamination (10,11). Additionally, contrast agents might be reserved for the evaluation of cerebral perfusion employing first-pass dynamic imaging techniques in AIS (12).

Consequently, different non-CE-MRA techniques have been proposed in the past (13-16). 2D/3D time-of-flight (TOF)-MRA enables the depiction of the cervical arteries without gadolinium contrast and is often used in clinical practice. Nevertheless, besides a long acquisition time, 2D/3D TOF-MRA shows limitations like sensitivity to respiratory and flow artifacts resulting from saturation and dephasing of flow spins if slow flow is present (17). Furthermore, TOF-MRA is impaired by an inferior image quality, decreased anatomic coverage, and most importantly by an overestimation of ICA stenosis compared to CE-MRA (18-20). Recently, alternate native MRA techniques have been proposed, including quiescent interval slice-selective (QISS)-MRA. QISS-MRA has shown promising results for imaging of the extracranial arteries (11,21-23) and other vascular territories (24). However, there are potential limitations, e.g., the 2D anisotropic acquisition and the dependency of the vessel signal on the inflow of spins from outside the saturation volume (11,21,22).

In 2019, the relaxation-enhanced angiography without contrast and triggering (REACT) technique was introduced by Yoneyama *et al*. The REACT sequence combines two prepulses [inversion recovery (IR) and T2 preparation] with a 3D dual-echo Dixon method for flow-independent 3D isotropic non-CE-MRA (25). By providing a concurrent delineation of arteries and veins, it has demonstrated promising results in the imaging of the thoracic vasculature (26-28) and other vascular territories (29). While the REACT sequence cannot depict the intracranial arteries (25,30), it has also shown a comparable image quality to CE-MRA for extracranial arteries in a recent study at 3T while providing a high sensitivity and specificity for the detection of stenosis of the extracranial ICA (30). However, given the small sample size of aforementioned study (n=35), the validity of these findings remains questionable, especially the sensitivity of vessel stenosis detection.

Thus, the purpose of this study in a large cohort of patients with AIS using CE-MRA as a reference standard was threefold: first, to assess the detection and classification

of extracranial ICA stenosis using the REACT sequence. Second, to study the concordance between both techniques regarding the assessment of adjacent plaques. Third, to assess the image quality of both MRA techniques focusing on the extracranial carotid arteries. We present the following article in accordance with the STARD reporting checklist (available at https://qims.amegroups.com/article/view/10.21037/qims-21-1122/rc).

Methods

The local institutional review board (Ethikkommission, Medizinische Fakultät der Universität zu Köln, No. 20-1067) approved this single-center study. Due to its retrospective design, the institutional review board waived the requirement for written informed consent. The study was conducted in accordance with the Declaration of Helsinki (as revised in 2013).

Patient population

The authors reviewed the institutional image data base at the University Hospital of Cologne for consecutive stroke MRI examinations between May 2019 and January 2020. Patients were included if they received a standardized stroke protocol [diagnosis of AIS based on a positive diffusion-weighted imaging (DWI)-lesion] which was acquired at 3T and included REACT and CE-MRA of the cervical arteries. Exclusion criteria were lack of scan data for any of extracranial MRAs, severe motion artifacts, pronounced pleural effusions, and technical failure of CE-MRA.

The following data were retrieved from the medical charts or monitored during MRI: age and gender of patients, risk factors for AIS, underlying disease for AIS, National Institutes of Health Stroke Scale [NIHSS, as determined by the treating neurologist upon admission (31)], affected vascular territory, present intracranial or extracranial haemorrhage, modified Rankin Scale [mRS (32)] at discharge, and sequelae of AIS.

MRI

All examinations were performed using a commercially available 3T MRI system (Philips Ingenia, Philips Healthcare, Best, The Netherlands) employing a standard 20-channel head and neck coil. The protocol consisted of axial fluid-attenuated IR sequences, DWI in the axial and coronal planes, axial susceptibility-weighted imaging, intracranial 3D TOF-MRA, REACT, and CE-MRA. In patients with suspected dissection, a native T1-weighted spectral presaturation with inversion recovery (SPIR) sequence was acquired covering the extracranial arteries from the aortic arch to the skull base.

The details of the applied extracranial MRA sequences have been described in detail elsewhere (30). In brief, a non-triggered flow-independent 3D isotropic REACT sequence was used for non-CE-MRA. REACT combines 50 ms T2 preparation and IR prepulses (to enhance the native blood signal with long T1 and T2) with a 3D mDIXON XD readout (to suppress the signal of the background and adjacent fat) (25). Data was acquired in the coronal plane; immediate image reconstruction was employed. Considering the fat-water artifacts of the mDIXON technique, water-only as well as in- and out-of-phase images were created (33,34). For CE-MRA, a non-triggered 3D gradient-echo T1 sequence was employed. After acquisition of an unenhanced MRA image as a mask, gadolinium-based contrast agent (Clariscan, GE Healthcare, Chicago, IL, USA; 0.2 mL/kg body weight) was injected in an antecubital vein (flow rate of 2 mL/s), succeeded by a 30-mL saline flush. As determined by a bolus-tracking sequence, data acquisition (coronal plane) was performed after arrival of contrast agent in the aortic arch. There was neither a table movement between bolus tracking and the acquisition data nor a subtraction of the CE-MRA images from the native scan with the latter enabling plaque assessment in CE-MRA by using the mask scan (4). Real-time reconstruction was employed.

For acceleration of acquisition of extracranial MRAs, Compressed SENSE (Philips Healthcare, Best, The Netherlands) was employed. This technique combines compressed sensing and parallel imaging based on SENSitivity Encoding (SENSE) (35-37). Data was acquired by employing a balanced variable density incoherent sampling patter within high-density in the k-space center and continuously decreasing sampling density towards the periphery of the k-space. An iterative L1 norm minimization ensuring data consistency and sparsity in the wavelet domain in combination with regularization by coil sensitivity distribution and SENSE parallel imaging was used for image reconstruction.

An acceleration factor of 4 was employed for REACT (scan time of 02:46 min) and an acceleration factor of 6 was used for CE-MRA (scan time of 01:08 min). *Table 1* summarizes the imaging parameters of both MRA sequences.

Table 1 Parameters of REACT and CE-MRA

Parameters	REACT	CE-MRA
Acquisition orientation	Coronal	Coronal
K-space trajectory	Cartesian	Cartesian
Field of view (FH × RL × AP) (mm^3)	320×400×80	320×280×80
Acquired voxel size (mm^3)	1.5×1.5×1.5	0.63×0.63×0.63
Reconstructed voxel size (mm^3)	0.625×0.625×0.750	0.5×0.5×0.5
Flip angle (°)	15	40
Repetition time (TR) (ms)	4.3	6.1
Echo time (TE, 1/2) (ms)	1.45/2.60	1.96
T2 preparation (ms)	50	n/a
Compressed SENSE factor	4	6
Temporal resolution (s)	n/a	1
Scan time (min)	02:46	01:08
Image reconstruction	Immediate	Real time

AP, anterior posterior; CE-MRA, contrast-enhanced magnetic resonance angiography; FH, feet head; n/a, not available; REACT, relaxation-enhanced angiography without contrast and triggering; RL, right left; SENSE, SENSitivity Encoding.

Image analysis

Three readers with different expertise levels in MRI [one radiologist with 3 years (UCI Hoyer), one radiologist with 4 years (F Fichter), and one neuroradiologist (N Abdullayev) with 7 years of experience in neurovascular MRI; R1, R2, and R3] independently reviewed the MRA images during separate sessions and in random order. For image analysis, reconstructed maximum intensity projections (MIPs, coronal plane, water-only of REACT; slab thickness: 6 mm, gap: 0 mm) and source images were evaluated using an IMPAX EE (release 20, Agfa HealthCare N.V., Mortsel, Belgium) workstation as in clinical routine. Readers could choose between the different reconstructions of the source images of the REACT sequence and were familiar with potential fat-water swapping artifacts in REACT. To minimize a potential recall bias, there was a period of at least four weeks between the analysis of REACT and CE-MRA datasets, respectively. Readers were free to alter window levelling and were blinded to clinical and patient data.

Assessment of image quality

Based on the delineation of the vessel as well as its signal intensity and its contrast to the adjacent tissue, readers assessed the vessel quality of MRA datasets employing a 5-point scale:

(I) Non-diagnostic, image quality insufficient for diagnosis;
(II) Poor, inferior image quality;
(III) Fair, mediocre image quality;
(IV) Good, image quality applicable for confident diagnosis;
(V) Excellent, image quality enabling highly reliable diagnosis.

Vessel quality was evaluated for the following arterial segments:

(I) Right common carotid artery (CCA);
(II) Cervical (C1) segment of the right ICA;
(III) Petrous (C2) segment of the right ICA;
(IV) Left CCA;
(V) C1 segment of the left ICA;
(VI) C2 segment of the left ICA.

When an occlusion was present, the vessel quality of the affected segment was not scored. Additionally, the radiologists rated the presence of artifacts (banding, pulsation, blurring, and parallel imaging reconstruction artifacts) in general and the noise affecting the extracranial carotid arteries employing the following 5-point scale: 1, non-diagnostic; 2, high effect on image quality; 3, moderate effect on image quality; 4, low effect on image quality; and 5, no effect on image quality.

Assessment of extracranial ICA stenosis

Readers assessed the MRA datasets for stenosis of the right and left extracranial ICA in the C1 segment based on the North American Symptomatic Carotid Endarterectomy Trial (NASCET) trial criteria using a scoring scale of 1–5:

(I) Grade 1: normal patency;
(II) Grade 2: stenosis, <50% of the vessel lumen;
(III) Grade 3: stenosis, 50–69% of the vessel lumen;
(IV) Grade 4: stenosis, ≥70–99% of the vessel lumen;
(V) Grade 5: complete vessel occlusion.

When multiple stenoses were present in the extracranial ICA, the most stenotic lesion was considered the diagnostic grade and used for further analysis. For each carotid bifurcation, the diagnostic confidence for the assessment of stenosis was rated using the following 3-point scoring system: 1 poor, 2 mediocre, and 3 excellent.

Detection of ICA plaques

In order to study for concordance between REACT and CE-MRA, radiologists evaluated the source images of MRA scans (which includes the mask scan of CE-MRA) for the presence of plaques of the right and left carotid bifurcation by responding to a dichotomous yes or no question. Additionally, readers classified plaques as either fully hypo- or partially hyperintense compared with the adjacent muscle. Readers were given exemplary teaching cases of hyper- and hypointense plaques before the original data set was handed out. Furthermore, readers were instructed to note their diagnostic confidence for the assessment of ICA plaques for each carotid bifurcation using the following 3-point scoring system: 1 poor, 2 mediocre, and 3 excellent.

Evaluation of fat-water swapping artifacts in REACT

For the assessment of potential artifacts, one radiologist (5 years of experience in neurovascular MRI) evaluated the acquired water maps for a potential signal loss and the concomitant in-phase image for the corresponding signal.

Statistical analysis

Statistical analysis was performed using JMP software (release 14.1.0, SAS Institute, Cary, NC, USA). Quantitative data are indicated as the mean ± standard deviation, unless noted otherwise. The data of image quality analysis are presented as the mean ± standard deviation and as the median with interquartile range and calculated by combining the measurements of all readers.

Given its high diagnostic accuracy, CE-MRA served as a reference standard for the sensitivity and specificity of REACT regarding its assessment of extracranial ICA stenosis (38). A stenosis grade ≥50% was interpreted as clinically relevant. The values for diagnostic confidence are given as the mean ± standard deviation and as the median with interquartile range. Wilcoxon tests were used to compare the image quality scores, the difference in assessment of ICA plaques between MRA sequences, and the diagnostic confidence for the assessment of ICA stenosis and plaques.

The interobserver agreement for the evaluation of image quality and the assessment of ICA stenosis was evaluated using Kendall's coefficient of concordance (Kendall's *W*). Cohen's Kappa was calculated to evaluate the agreement between REACT and CE-MRA in the grading of ICA stenosis (0.01–0.20 slight, 0.21–0.40 fair, 0.41–0.60 moderate, 0.61–0.80 substantial, and 0.81–0.99 almost perfect). Statistical significance was set to $P<0.05$.

Results

Study population and baseline characteristics

One hundred and twenty-five potential patients could be identified. Of these, 20 patients were excluded due to lack of MRA sequences, severe artifacts, technical failure, and pleural effusions. *Figure 1* depicts a workflow for inclusion and exclusion of study participants. Consequently, 105 patients were included in this study (65.27±18.74 years; range, 5–92 years; 42 females). *Table 2* provides detailed patient and stroke characteristics.

Image quality

Each reader evaluated 210 datasets (105 for REACT and 105 for CE-MRA, respectively), resulting in 1,260 vessel segments for analysis. For all vessels combined, the vessel quality of the extracranial carotid arteries was comparable between both techniques {4.61±0.66 *vs.* 4.58±0.68; 5 [4–5] *vs.* 5 [4–5], P=0.0299}. Of note, CE-MRA showed a lower median for both sides of the CCA {4 [4–5] *vs.* 5 [4–5], P=0.0050 and P=0.0133, respectively}. Regarding the presence of artifacts, there was no significant difference between both MRA techniques {5 [4–5] *vs.* 5 [4–5], P=0.0847} whereas REACT showed a lower image noise {5 [4–5] *vs.* 4 [4–5], P<0.0001}. Detailed results of image quality assessment are provided in *Table 3*.

For both MRA methods, there was a moderate

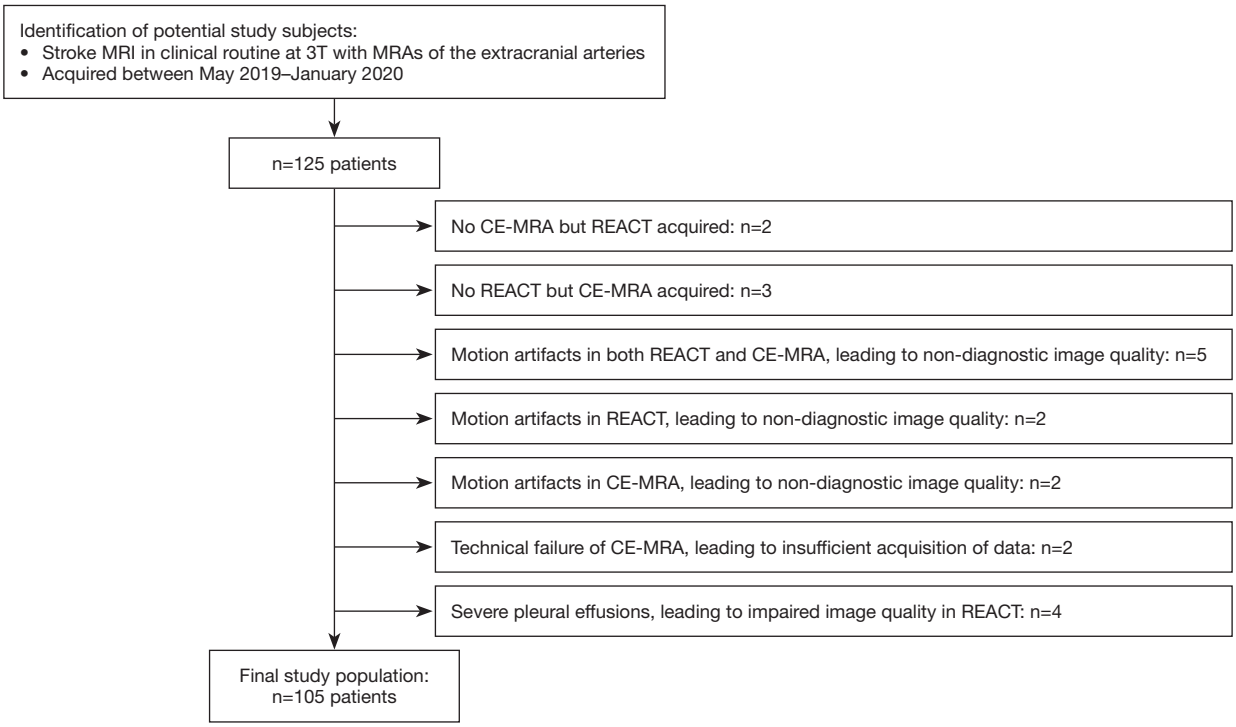

Figure 1 Workflow for inclusion and exclusion of patients. MRI, magnetic resonance imaging; CE-MRA, contrast-enhanced magnetic resonance angiography; REACT, relaxation-enhanced angiography without contrast and triggering.

agreement on all image quality criteria as outlined in *Table 4*.

Assessment of extracranial ICA stenosis

For all readers combined and for any type of stenosis, REACT provided a sensitivity of 89.8% (95% CI: 84.9–93.6%) with a corresponding specificity of 95.2% (95% CI: 92.7–97.1%). For clinically relevant stenosis (≥50%), REACT yielded an overall sensitivity of 93.5% (95% CI: 86.5–97.6%) and a specificity of 95.8% (95% CI: 90.4–98.6%). Single reviewer results for sensitivity and specificity are provided in Table S1. Table S2 lists the exact numbers of stenosis found per grade.

Interobserver agreement for REACT was almost perfect (Kendall's *W* 0.9). Further, REACT achieved an almost perfect accordance with CE-MRA regarding the grading of disease [Cohen's Kappa 0.9 (95% CI: 0.88–0.93)].

REACT showed a diagnostic confidence of 2.8±0.5 {3 [3–3]; R1: 2.9±0.3, 3 [3–3]; R2: 2.7±0.5, 3 [2–3]; and R3: 2.8±0.4, 3 [3–3]} for the assessment of ICA stenosis with CE-MRA yielding a mean of 2.7±0.5 {3 [2–3]; R1: 2.9±0.3, 3 [2–3]; R2: 2.6±0.6, 3 [2–3]; and R3: 2.7±0.5, 3 [2–3]; overall P=0.03}.

Figures 2-4 give illustrative examples of the depiction of stenosis of the extracranial ICA using REACT and CE-MRA.

Detection of ICA plaques

Overall, readers detected more plaques using REACT (R1: n=49 plaques, 23.3% of analyzed carotid bifurcations; R2: n=59, 28.1%; and R3: n=64, 30.5%) compared to CE-MRA (R1: n=41, 19.5%; R2: n=46, 21.9%; and R3: n=56, 26.7%; overall: n=57.3, 27.3% *vs.* n=47.7, 22.7%, P<0.001). In REACT, readers were able to detect more plaques of hyperintense signal (R1: n=12, 24.5% of detected plaques; R2: n=12, 20.3%; and R3: n=13, 20.3%) than in CE-MRA (R1: n=5, 12.2%; R2: n=4, 8.7%; and R3: n=8, 14.3%; overall: 12.3, 21.5% *vs.* 5.7, 11.9%, P=0.02).

Additionally, REACT {R1: 2.8±0.4, 3 [3–3]; R2: 2.7±0.5, 3 [2–3]; and R3: 2.8±0.4, 3 [3–3]} yielded a higher diagnostic confidence than CE-MRA {R1: 2.7±0.6, 3 [3–3]; R2: 2.4±0.8, 3 [2–3]; and R3: 2.6±0.5, 3 [2–3]; overall: 2.8±0.5, 3 [3–3] *vs.* 2.6±0.7, 3 [2–3], P<0.001} for plaque assessment.

Illustrative examples of the assessment of ICA plaques using REACT and CE-MRA are provided in *Figures 5-7*.

Table 2 Patient and stroke characteristics

Characteristics	Value
Age (years), mean ± SD	65.27±18.74
Gender, n (%)	
Female	42 (40.00)
Male	63 (60.00)
Risk factors, n (%)	
Hypertension	62 (59.05)
Diabetes mellitus	23 (21.90)
Dyslipidemia	19 (18.1)
Smoking	18 (17.14)
Previous stroke/TIA	27 (25.71)
Atrial fibrillation	21 (20.00)
Underlying disease, n (%)	
Atherosclerosis	57 (54.29)
Small vessel disease	26 (24.76)
Cardiac	34 (32.38)
Dissection	7 (6.67)
NIHSS upon admission, mean ± SD	4.30±3.84
Vascular territory, n (%)	
Anterior circulation	74 (70.48)
Posterior circulation	41 (39.05)
Bleeding, n (%)	
Intracranial	15 (14.29)
Extracranial	3 (2.86)
mRS at discharge, mean ± SD	2.07±1.61
Sequelae, n (%)	
Paralysis	42 (40.00)
Aphasia	6 (5.71)
Dysarthria	12 (11.43)
Hypesthesia	16 (15.24)
Dizziness	3 (2.86)
Impaired eye movement/visual neglect	18 (17.14)

TIA, transient ischemic attack; NIHSS, National Institutes of Health Stroke Scale; mRS, modified Rankin Scale; SD, standard deviation.

Fat-water swapping artifacts in REACT

In 36 of 105 patients (34.3%), fat-water swapping artifacts were noticed in water-only maps of REACT. These artifacts were observed at the proximal subclavian artery (36 cases, left) and the proximal CCA (four cases, left). When assessing the corresponding in-phase images, a high vessel signal was present in every case.

Discussion

In this work, we investigated the diagnostic performance of a novel non-CE-MRA (REACT) for the depiction of extracranial carotid arteries by comparing the detection of extracranial ICA stenosis with concomitant plaques and the image quality of REACT with CE-MRA in a large patient cohort with AIS. The three major findings of the study are the following: REACT provides a high sensitivity and specificity for extracranial ICA stenosis, particularly for clinically relevant stenosis. Without the use of gadolinium-based contrast agents or triggering, readers were able to detect more plaques in REACT compared to CE-MRA. In less than three min, REACT achieved to CE-MRA comparable vessel quality of the extracranial carotid arteries while yielding a lower image noise.

In this large cohort, REACT yielded a high sensitivity (90%) and specificity (95%) for extracranial ICA stenosis, particularly for clinically relevant pathologies (sensitivity of 94% and specificity of 96%) while providing similar diagnostic confidence as the reference standard CE-MRA. These findings are confirming the results of aforementioned previous study (30) and are in line with reported sensitivities and specificities of other non-contrast MRA sequences as QISS-MRA [up to 86% and 90%, respectively (11,22)]. For grading of disease, REACT showed an almost perfect agreement with CE-MRA [comparable to QISS-MRA (21,22)] whereas TOF-MRA tends to overestimate the degree of extracranial ICA stenosis (19-22), another limitation making it widely unsuitable for the assessment of extracranial arteries.

Using REACT, readers were able to detect more plaques adjacent to the carotid bifurcation compared to CE-MRA. Of note, the CE-MRA technique of the present study, opposed to other techniques, which perform a subtraction

Table 3 Image quality scores of REACT and CE-MRA

Vessel quality	REACT		CE-MRA		P value
	Median [IQR]	Mean ± SD	Median [IQR]	Mean ± SD	
Right side					
CCA	5 [4–5]	4.45±0.74	4 [4–5]	4.36±0.73	0.0050*
ICA, C1 segment	5 [5–5]	4.68±0.65	5 [4–5]	4.67±0.64	0.6385
ICA, C2 segment	5 [5–5]	4.70±0.60	5 [5–5]	4.75±0.52	0.3609
Left side					
CCA	5 [4–5]	4.43±0.75	4 [4–5]	4.33±0.76	0.0133*
ICA, C1 segment	5 [4.25–5]	4.70±0.57	5 [4–5]	4.64±0.68	0.5137
ICA, C2 segment	5 [5–5]	4.70±0.73	5 [4–5]	4.74±0.73	0.2291
Overall	5 [4–5]	4.61±0.66	5 [4–5]	4.58±0.68	0.0299*
Artifacts	5 [4–5]	4.51±0.70	5 [4–5]	4.44±0.73	0.0847
Noise	5 [4–5]	4.43±0.67	4 [4–5]	4.25±0.71	<0.0001*

*, statistical significance. Scoring scales of 1–5 were used, 1 being non-diagnostic. REACT, Relaxation-Enhanced Angiography without Contrast and Triggering; CE-MRA, contrast-enhanced magnetic resonance angiography; CCA, common carotid artery; ICA, internal carotid artery; IQR, interquartile range; SD, standard deviation.

Table 4 Interobserver agreement for CE-MRA and REACT, assessed by Kendall's *W* (0.01–0.2 slight, 0.21–0.4 fair, 0.41–0.6 moderate, 0.61–0.8 substantial, and 0.81–0.99 almost perfect)

Criterion	CE-MRA	REACT
Vessel quality	0.48	0.52
Artifacts	0.52	0.58
Noise	0.51	0.46

CE-MRA, contrast-enhanced magnetic resonance angiography; REACT, relaxation-enhanced angiography without contrast and triggering.

of the pre-contrast scan (39), allows an evaluation of the supraaortic arteries including the mask scan, which enables plaque assessment in CE-MRA (4-6). The slightly improved detection of plaques overall in REACT can be explained by the fact that although applying magnetization-prepared (STIR and T2 preparation prepulses) mDIXON for background suppression, the signal of the background is still higher than in CE-MRA, which facilitates the detection of plaques. Additionally, the REACT sequence uses STIR for magnetization preparation, which, together with the T2 preparation prepulse, creates an image of T2-/T1-weighted contrast (25). This feature may explain why readers were able to detect more plaques with partially hyperintense signal in REACT compared to CE-MRA. A hyperintense plaque in REACT may refer to intraplaque hemorrhage or ulcerated plaques, respectively, when comparing this signal intensity to the T1-weighted SPIR sequence in *Figure 5*. Although not approximating to true plaque imaging, which is time consuming and still widely unsuitable for clinical routine, these findings are important since the REACT sequence may be suitable to identify unstable plaques that are at risk of thromboembolic events at a higher sensitivity than other non-CE-MRA sequences. In this context, T1-weighted TOF-MRA has shown inferior detection of intraplaque hemorrhage than CE-MRA when including the mask scan of the latter (4,5).

REACT, as indicated in a prior study with a small patient population (30), provided an image quality of the extracranial carotid arteries based on the subjective evaluation of vessel delineation, signal, and contrast which was comparable to high-resolution CE-MRA. With CE-MRA being occasionally hampered by pulsation artifacts, which are more pronounced at the aortic arch and its branches, REACT showed a superior vessel quality for the CCA of both sides. While CE-MRA tends to allow for better vessel delineation, most likely given its high submillimetre isotropic resolution, the REACT sequence counterbalances this limited spatial resolution by providing a higher vessel signal and contrast to the adjacent soft tissue (30). Furthermore, the

Figure 2 Maximum intensity projections, angulated to the right carotid bifurcation (slab thickness: 20 mm), in a 77-year-old woman with anterior circulation stroke showing an extracranial internal carotid artery stenosis (wide arrows, grade 2) in REACT (water-only reconstructions) and CE-MRA. Dagger: concomitant moderate stenosis of the external carotid artery. REACT, relaxation-enhanced angiography without contrast and triggering; CE-MRA, contrast-enhanced magnetic resonance angiography.

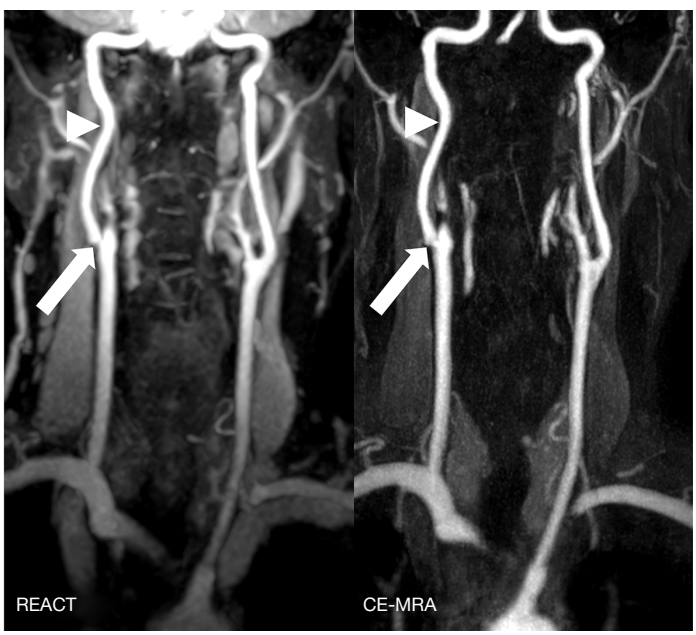

Figure 3 Maximum intensity projections in coronal orientation (slab thickness: 15 mm) in a 63-year-old man with ischemia of the right postcentral gyrus depicting an extracranial internal carotid artery stenosis (wide arrows, up to grade 3) in REACT (water-only reconstructions) and CE-MRA. Due to pulsation artifacts, CE-MRA shows a blurred vessel delineation at the aortic arch compared to REACT. Additionally, REACT yields a high vessel signal intensity at the internal carotid arteries compared to CE-MRA (arrowheads). REACT, relaxation-enhanced angiography without contrast and triggering; CE-MRA, contrast-enhanced magnetic resonance angiography.

Figure 4 Maximum intensity projections, angulated to the left carotid bifurcation (slab thickness: 20 mm), in a 65-year-old woman with ischemia of the left frontal lobe depicting a multisegmental stenosis of the extracranial internal carotid artery (wide arrows) with improved delineation of the stenosis in REACT (water-only reconstructions) compared to a blurred appearance in CE-MRA due to a higher noise. REACT, relaxation-enhanced angiography without contrast and triggering; CE-MRA, contrast-enhanced magnetic resonance angiography.

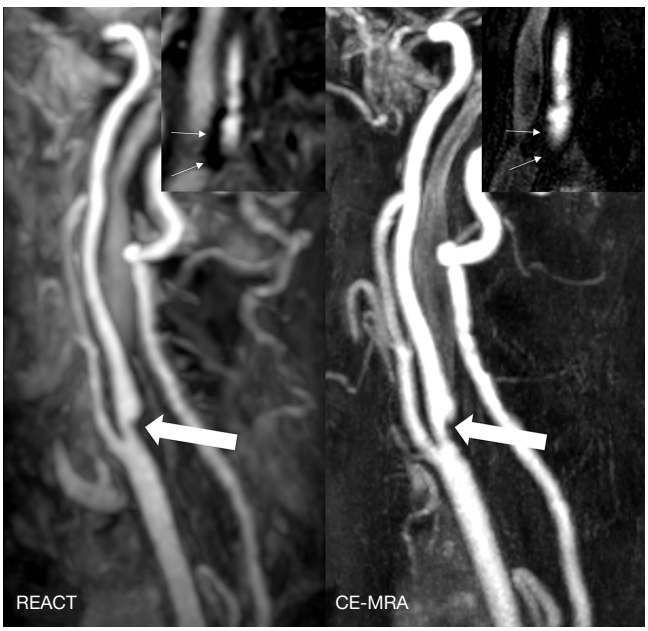

Figure 5 Maximum intensity projections, angulated to the left carotid bifurcation (slab thickness: 20 mm), in an 81-year-old woman with ischemia of the left precentral gyrus showing an extracranial internal carotid artery stenosis (wide arrows, grade 3) in REACT (water-only reconstructions) and CE-MRA. Additionally, source images of REACT (coronal view) reveal a hypointense plaque (thin arrows) of the contralateral carotid bifurcation, being of impaired visibility in CE-MRA. REACT, relaxation-enhanced angiography without contrast and triggering; CE-MRA, contrast-enhanced magnetic resonance angiography.

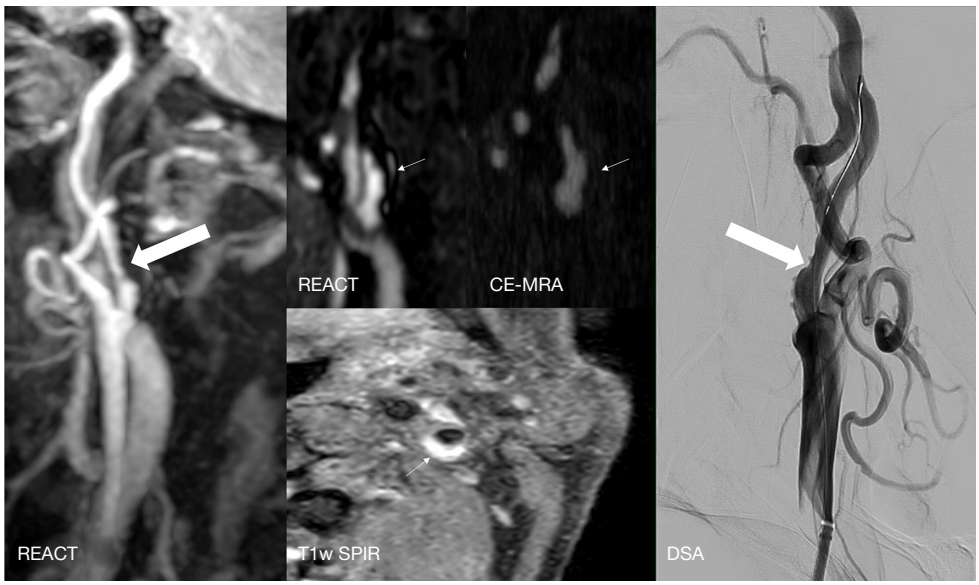

Figure 6 A 76-year-old man with left hemispheric watershed infarction. Maximum intensity projections, angulated to the left carotid bifurcation (slab thickness: 20 mm) of REACT (water-only) indicate an extracranial internal carotid artery stenosis (wide white arrow, grade 3). Source images in the coronal plane of REACT (water-only) reveal a partially hyperintense concomitant plaque (thin arrows), whereas the plaque and its hyperintensity is barely visible in the source images of CE-MRA. Axial T1w SPIR sequence depicts a corresponding ulcerated plaque with vessel wall hematoma (thin arrow), which was confirmed and treated with a carotid wall stent in the subsequently performed DSA (wide white arrow). REACT, relaxation-enhanced angiography without contrast and triggering; CE-MRA, contrast-enhanced magnetic resonance angiography; T1w, T1-weighted; SPIR, spectral presaturation with inversion recovery; DSA, digital subtraction angiography.

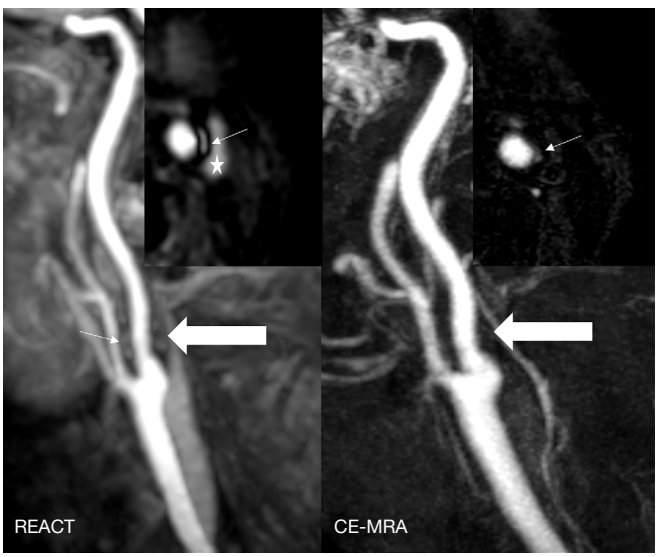

Figure 7 Maximum intensity projections, angulated to the left carotid bifurcation (slab thickness: 15 mm), in a 71-year-old man with multiple embolic ischemia of the left precentral gyrus indicating an extracranial internal carotid artery stenosis (wide arrows, grade 2) in REACT (water-only) and CE-MRA. Source images of REACT (axial plane) clearly reveal an adjacent plaque of predominantly hyperintense signal, while its visibility is hampered in CE-MRA (thin arrows). *, internal jugular vein. REACT, relaxation-enhanced angiography without contrast and triggering; CE-MRA, contrast-enhanced magnetic resonance angiography.

REACT sequence yields a lower image noise than CE-MRA, most likely given its longer acquisition time, their technical differences, and their different spatial resolution (1.5 *vs.* 0.63 mm^3 acquired voxel size).

Compared to 2D QISS-MRA, the mDIXON readout enables the acquisition of high-resolution 3D isotropic datasets over a large field of view in REACT and combines advantages of SSFP with the suppression of background and fat while providing a fat/water separation (25,33). Furthermore, the 3D readout enables image reconstruction in any arbitrary direction of space, which facilitates the assessment of vascular pathologies, e.g., the presence of ICA stenosis and plaques. Given their flow dependency and concomitant artifacts, the image quality of TOF- and QISS-MRA may be impaired, which explains the overestimation of TOF-MRA for ICA stenosis due to signal intensity saturation of low flow distal to high-grade stenosis (14,17,18). On the contrary, REACT is flow-independent and enhances blood vessels given their different T1 and T2 relaxation times (25). Furthermore, the REACT sequence does not require any triggering which is beneficial in daily clinical practice given that stroke imaging is generally performed without pulse or cardiac synchronization (25).

3D TOF-MRA and ungated QISS-MRA require a long acquisition time of up to seven min to depict the extracranial arteries (11,21,22). On the contrary, REACT enables a faster depiction of the extracranial arteries (in less than three min) when accelerating its acquisition with Compressed SENSE, which has already indicated promising results in different fields of MRI (40,41). Using deep neural network–based image processing, the acquisition time of QISS-MRA can be reduced to less than three min (23). However, besides unknown reconstruction times, the required additional central processing unit cluster limits its feasibility for other centers (23). In contrast, the Compressed SENSE technique was fully integrated into the clinical system and does not require extensive reconstruction times or postprocessing while being performed with the standard hardware as provided by the manufacturer of the MRI system (30). Given its short acquisition time, REACT is also faster to acquire than the CE-MRA sequence used in the present study when considering the unenhanced scan, the required time for bolus-tracking, and the necessary preparation of the patient for the application of contrast agent. With CE-MRA being dependent on the accurate acquisition of data with respect to the arrival of the contrast agent (10,11), REACT can be acquired as often as necessary, being feasible for patients requiring follow-up imaging without the additional cost of contrast agents.

As a major limitation and disadvantage compared to QISS- and TOF-MRA, REACT, which has a selectivity for tissues with long T1 and T2, cannot depict the intracranial arteries given the long T1 and T2 of the cerebrospinal fluid (25,30). Consequently, REACT is not suitable for patients with severe pleural effusions, which were excluded from this study. Nevertheless, when combining TOF-MRA and REACT for the imaging of intra- and extracranial arteries, the supraaortic arteries can be depicted sufficiently in the setting of AIS without the application of contrast. Since REACT showed fat-water swapping artifacts in more than a third of patients, readers must be aware of this important artifact when using the sequence. However, the corresponding in-phase reconstructions yielded a bright vessel signal, clarifying the dropout as artificial. Whereas QISS- and TOF-MRA provide scans of minor or no contamination by venous vessels (11,21,22), REACT provides a simultaneous depiction of arteries and veins, which is beneficial in the imaging of large thoracic vessels but potentially of disadvantage for the imaging of the extracranial arteries where vessels are smaller (25). However, a high arterial signal is provided when choosing a low flip angle (15°) and by the combination of IR and T2 preparation prepulses for magnetization preparation with the vessel signal of REACT being dependent on the O2 saturation of the vessels, which leads to a higher signal intensity of arteries. Additionally, the combination of the mDIXON XD readout with magnetization preparation leads to a higher arterial signal, which enables a clear separation of arterial and venous vessels as well as of adjacent tissue (25).

Limitations

Besides being a retrospective single-centre investigation, there were limitations to this study. First, there was no standard of reference for the assessment of ICA plaques and the evaluation of their signal intensity with both CE-MRA and REACT not approximating to true plaque imaging. Hence, the results regarding plaque detection and characterization in REACT might carry a bias and even an oversensitivity, especially regarding hyperintense plaques and their suspected instability. Further studies, either using additional plaque imaging sequences or T1-weighted SPIR in a broad patient cohort to further evaluate the potential use of REACT for the assessment of stable and unstable plaques with intraplaque hemorrhage are

required to confirm the observational findings of the present study. In this regard, additional studies with patients referred for carotid endarterectomy may be of interest in the future to provide a histopathological standard of reference. Second, no comparison of REACT to digital subtraction angiography (DSA), the gold standard for imaging of supraaortic arteries, was conducted in the present work. Third, since this study intended to focus on the clinical performance of the REACT sequence in terms of stenosis and plaque assessment, we did not choose to conduct an objective evaluation of image quality based on signal- and contrast-to-noise ratios. However, as shown in aforementioned previous study focusing on image quality (30), REACT showed higher vessel signal and contrast than CE-MRA based on subjective and objective evaluations. Fourth, full blinding of the readers to the type of MRA was not feasible given the difference in appearance of MRAs, which could have influenced the results. Fifth, the Compressed SENSE acceleration factor of REACT was chosen based on our clinical experience with the sequence and not after profound investigation of different undersampling factors. Therefore, higher acceleration factors and a faster acquisition may be feasible and desirable in AIS and should be investigated further.

Conclusions

In a large patient cohort with AIS, REACT provides high sensitivity and specificity for extracranial ICA stenosis, potentially improved depiction of plaques, and comparable vessel quality compared to the reference standard CE-MRA.

Acknowledgments

Clinician Scientist position is supported by the Deans Office, Faculty of Medicine, University of Cologne.
Funding: None.

Footnote

Reporting Checklist: The authors have completed the STARD reporting checklist. Available at https://qims.amegroups.com/article/view/10.21037/qims-21-1122/rc

Conflicts of Interest: All authors have completed the ICMJE uniform disclosure form (available at https://qims.amegroups.com/article/view/10.21037/qims-21-1122/coif). SL, NA, and RJG report that they received research support from Philips Healthcare. JPG and JB are on the speaker's bureau of Siemens Healthineers. JPG reports that he received payment for expert testimony from Siemens Healthineers. DM, JB, and LP are on the speaker's bureau of Philips Healthcare. KW is an employee of Philips Healthcare and reports that he holds stock of Philips Healthcare. The other authors have no conflicts of interest to declare.

Ethical Statement: The authors are accountable for all aspects of the work in ensuring that questions related to the accuracy or integrity of any part of the work are appropriately investigated and resolved. The study was conducted in accordance with the Declaration of Helsinki (as revised in 2013). This retrospective study was approved by the Ethikkommission, Medizinische Fakultät der Universität zu Köln (No. 20-1067). Written informed consent was waived due to the retrospective character of the study.

References

1. Powers WJ, Rabinstein AA, Ackerson T, Adeoye OM, Bambakidis NC, Becker K, Biller J, Brown M, Demaerschalk BM, Hoh B, Jauch EC, Kidwell CS, Leslie-Mazwi TM, Ovbiagele B, Scott PA, Sheth KN, Southerland AM, Summers DV, Tirschwell DL. Guidelines for the Early Management of Patients With Acute Ischemic Stroke: 2019 Update to the 2018 Guidelines for the Early Management of Acute Ischemic Stroke: A Guideline for Healthcare Professionals From the American Heart Association/American Stroke Association. Stroke 2019;50:e344-418.
2. Flaherty ML, Kissela B, Khoury JC, Alwell K, Moomaw CJ, Woo D, Khatri P, Ferioli S, Adeoye O, Broderick JP, Kleindorfer D. Carotid artery stenosis as a cause of stroke. Neuroepidemiology 2013;40:36-41.

3. Phan T, Huston J 3rd, Bernstein MA, Riederer SJ, Brown RD Jr. Contrast-enhanced magnetic resonance angiography of the cervical vessels: experience with 422 patients. Stroke 2001;32:2282-6.
4. Qiao Y, Etesami M, Malhotra S, Astor BC, Virmani R, Kolodgie FD, Trout HH 3rd, Wasserman BA. Identification of intraplaque hemorrhage on MR angiography images: a comparison of contrast-enhanced mask and time-of-flight techniques. AJNR Am J Neuroradiol 2011;32:454-9.
5. Demarco JK, Ota H, Underhill HR, Zhu DC, Reeves MJ, Potchen MJ, Majid A, Collar A, Talsma JA, Potru S, Oikawa M, Dong L, Zhao X, Yarnykh VL, Yuan C. MR carotid plaque imaging and contrast-enhanced MR angiography identifies lesions associated with recent ipsilateral thromboembolic symptoms: an in vivo study at 3T. AJNR Am J Neuroradiol 2010;31:1395-402.
6. Etesami M, Hoi Y, Steinman DA, Gujar SK, Nidecker AE, Astor BC, Portanova A, Qiao Y, Abdalla WM, Wasserman BA. Comparison of carotid plaque ulcer detection using contrast-enhanced and time-of-flight MRA techniques. AJNR Am J Neuroradiol 2013;34:177-84.
7. Kuo PH, Kanal E, Abu-Alfa AK, Cowper SE. Gadolinium-based MR contrast agents and nephrogenic systemic fibrosis. Radiology 2007;242:647-9.
8. Jung JW, Kang HR, Kim MH, Lee W, Min KU, Han MH, Cho SH. Immediate hypersensitivity reaction to gadolinium-based MR contrast media. Radiology 2012;264:414-22.
9. Kanda T, Matsuda M, Oba H, Toyoda K, Furui S. Gadolinium Deposition after Contrast-enhanced MR Imaging. Radiology 2015;277:924-5.
10. Menke J. Carotid MR angiography with traditional bolus timing: clinical observations and Fourier-based modelling of contrast kinetics. Eur Radiol 2009;19:2654-62.
11. Peters S, Huhndorf M, Jensen-Kondering U, Larsen N, Koktzoglou I, Edelman RR, Graessner J, Both M, Jansen O, Salehi Ravesh M. Non-Contrast-Enhanced Carotid MRA: Clinical Evaluation of a Novel Ungated Radial Quiescent-Interval Slice-Selective MRA at 1.5T. AJNR Am J Neuroradiol 2019;40:1529-37.
12. Copen WA, Schaefer PW, Wu O. MR perfusion imaging in acute ischemic stroke. Neuroimaging Clin N Am 2011;21:259-83, x.
13. Kramer H, Runge VM, Morelli JN, Williams KD, Naul LG, Nikolaou K, Reiser MF, Wintersperger BJ. Magnetic resonance angiography of the carotid arteries: comparison of unenhanced and contrast enhanced techniques. Eur Radiol 2011;21:1667-76.
14. Miyazaki M, Lee VS. Nonenhanced MR angiography. Radiology 2008;248:20-43.
15. Katsuki M, Narita N, Ishida N, Sugawara K, Watanabe O, Ozaki D, Sato Y, Kato Y, Jia W, Tominaga T. Usefulness of 3 Tesla Ultrashort Echo Time Magnetic Resonance Angiography (UTE-MRA, SILENT-MRA) for Evaluation of the Mother Vessel after Cerebral Aneurysm Clipping: Case Series of 19 Patients. Neurol Med Chir (Tokyo) 2021;61:193-203.
16. Nishikawa A, Kakizawa Y, Wada N, Yamamoto Y, Katsuki M, Uchiyama T. Usefulness of Pointwise Encoding Time Reduction with Radial Acquisition and Subtraction-Based Magnetic Resonance Angiography after Cerebral Aneurysm Clipping. World Neurosurg X 2020;9:100096.
17. Debrey SM, Yu H, Lynch JK, Lövblad KO, Wright VL, Janket SJ, Baird AE. Diagnostic accuracy of magnetic resonance angiography for internal carotid artery disease: a systematic review and meta-analysis. Stroke 2008;39:2237-48.
18. Boujan T, Neuberger U, Pfaff J, Nagel S, Herweh C, Bendszus M, Möhlenbruch MA. Value of Contrast-Enhanced MRA versus Time-of-Flight MRA in Acute Ischemic Stroke MRI. AJNR Am J Neuroradiol 2018;39:1710-6.
19. Weber J, Veith P, Jung B, Ihorst G, Moske-Eick O, Meckel S, Urbach H, Taschner CA. MR angiography at 3 Tesla to assess proximal internal carotid artery stenoses: contrast-enhanced or 3D time-of-flight MR angiography? Clin Neuroradiol 2015;25:41-8.
20. Platzek I, Sieron D, Wiggermann P, Laniado M. Carotid Artery Stenosis: Comparison of 3D Time-of-Flight MR Angiography and Contrast-Enhanced MR Angiography at 3T. Radiol Res Pract 2014;2014:508715.
21. Koktzoglou I, Murphy IG, Giri S, Edelman RR. Quiescent interval low angle shot magnetic resonance angiography of the extracranial carotid arteries. Magn Reson Med 2016;75:2072-7.
22. Koktzoglou I, Aherne EA, Walker MT, Meyer JR, Edelman RR. Ungated nonenhanced radial quiescent interval slice-selective (QISS) magnetic resonance angiography of the neck: Evaluation of image quality. J Magn Reson Imaging 2019;50:1798-807.
23. Koktzoglou I, Huang R, Ong AL, Aouad PJ, Aherne EA, Edelman RR. Feasibility of a sub-3-minute imaging strategy for ungated quiescent interval slice-selective MRA of the extracranial carotid arteries using radial k-space sampling and deep learning-based image processing. Magn Reson Med 2020;84:825-37.

24. Edelman RR, Silvers RI, Thakrar KH, Metzl MD, Nazari J, Giri S, Koktzoglou I. Nonenhanced MR angiography of the pulmonary arteries using single-shot radial quiescent-interval slice-selective (QISS): a technical feasibility study. J Cardiovasc Magn Reson 2017;19:48.
25. Yoneyama M, Zhang S, Hu HH, Chong LR, Bardo D, Miller JH, Toyonari N, Katahira K, Katsumata Y, Pokorney A, Ng CK, Kouwenhoven M, Van Cauteren M. Free-breathing non-contrast-enhanced flow-independent MR angiography using magnetization-prepared 3D non-balanced dual-echo Dixon method: A feasibility study at 3 Tesla. Magn Reson Imaging 2019;63:137-46.
26. Pennig L, Wagner A, Weiss K, Lennartz S, Grunz JP, Maintz D, Laukamp KR, Hickethier T, Naehle CP, Bunck AC, Doerner J. Imaging of the pulmonary vasculature in congenital heart disease without gadolinium contrast: Intraindividual comparison of a novel Compressed SENSE accelerated 3D modified REACT with 4D contrast-enhanced magnetic resonance angiography. J Cardiovasc Magn Reson 2020;22:8.
27. Pennig L, Wagner A, Weiss K, Lennartz S, Huntgeburth M, Hickethier T, Maintz D, Naehle CP, Bunck AC, Doerner J. Comparison of a novel Compressed SENSE accelerated 3D modified relaxation-enhanced angiography without contrast and triggering with CE-MRA in imaging of the thoracic aorta. Int J Cardiovasc Imaging 2021;37:315-29.
28. Isaak A, Luetkens JA, Faron A, Endler C, Mesropyan N, Katemann C, Zhang S, Kupczyk P, Kuetting D, Attenberger U, Dabir D. Free-breathing non-contrast flow-independent cardiovascular magnetic resonance angiography using cardiac gated, magnetization-prepared 3D Dixon method: assessment of thoracic vasculature in congenital heart disease. J Cardiovasc Magn Reson 2021;23:91.
29. Tan EJ, Zhang S, Tirukonda P, Chong LR. REACT - A novel flow-independent non-gated non-contrast MR angiography technique using magnetization-prepared 3D non-balanced dual-echo dixon method: Preliminary clinical experience. Eur J Radiol Open 2020;7:100238.
30. Pennig L, Kabbasch C, Hoyer UCI, Lennartz S, Zopfs D, Goertz L, Laukamp KR, Wagner A, Grunz JP, Doerner J, Persigehl T, Weiss K, Borggrefe J. Relaxation-Enhanced Angiography Without Contrast and Triggering (REACT) for Fast Imaging of Extracranial Arteries in Acute Ischemic Stroke at 3 T. Clin Neuroradiol 2021;31:815-26.
31. Lyden P. Using the National Institutes of Health Stroke Scale: A Cautionary Tale. Stroke 2017;48:513-9.
32. van Swieten JC, Koudstaal PJ, Visser MC, Schouten HJ, van Gijn J. Interobserver agreement for the assessment of handicap in stroke patients. Stroke 1988;19:604-7.
33. Eggers H, Brendel B, Duijndam A, Herigault G. Dual-echo Dixon imaging with flexible choice of echo times. Magn Reson Med 2011;65:96-107.
34. Ma J. Dixon techniques for water and fat imaging. J Magn Reson Imaging 2008;28:543-58.
35. Lustig M, Donoho D, Pauly JM. Sparse MRI: The application of compressed sensing for rapid MR imaging. Magn Reson Med 2007;58:1182-95.
36. Pruessmann KP, Weiger M, Scheidegger MB, Boesiger P. SENSE: sensitivity encoding for fast MRI. Magn Reson Med 1999;42:952-62.
37. Liang D, Liu B, Wang J, Ying L. Accelerating SENSE using compressed sensing. Magn Reson Med 2009;62:1574-84.
38. Willinek WA, von Falkenhausen M, Born M, Gieseke J, Höller T, Klockgether T, Textor HJ, Schild HH, Urbach H. Noninvasive detection of steno-occlusive disease of the supra-aortic arteries with three-dimensional contrast-enhanced magnetic resonance angiography: a prospective, intra-individual comparative analysis with digital subtraction angiography. Stroke 2005;36:38-43.
39. Riederer SJ, Stinson EG, Weavers PT. Technical Aspects of Contrast-enhanced MR Angiography: Current Status and New Applications. Magn Reson Med Sci 2018;17:3-12.
40. Bratke G, Rau R, Weiss K, Kabbasch C, Sircar K, Morelli JN, Persigehl T, Maintz D, Giese D, Haneder S. Accelerated MRI of the Lumbar Spine Using Compressed Sensing: Quality and Efficiency. J Magn Reson Imaging 2019;49:e164-75.
41. Pennig L, Lennartz S, Wagner A, Sokolowski M, Gajzler M, Ney S, Laukamp KR, Persigehl T, Bunck AC, Maintz D, Weiss K, Naehle CP, Doerner J. Clinical application of free-breathing 3D whole heart late gadolinium enhancement cardiovascular magnetic resonance with high isotropic spatial resolution using Compressed SENSE. J Cardiovasc Magn Reson 2020;22:89.

Cite this article as: Hoyer UCI, Lennartz S, Abdullayev N, Fichter F, Jünger ST, Goertz L, Laukamp KR, Gertz RJ, Grunz JP, Hohmann C, Maintz D, Persigehl T, Kabbasch C, Borggrefe J, Weiss K, Pennig L. Imaging of the extracranial internal carotid artery in acute ischemic stroke: assessment of stenosis, plaques, and image quality using relaxation-enhanced angiography without contrast and triggering (REACT). Quant Imaging Med Surg 2022;12(7):3640-3654. doi: 10.21037/qims-21-1122

